JMEPEG (2018) 27:1103–1108
https://doi.org/10.1007/s11665-018-3139-7

1059-9495/$19.00

Dendritic Zinc Growth in Acid Electrolyte: Effect of the pH

Leandro N. Bengoa, Paola Pary, Pablo R. Seré, M. Susana Conconi, and Walter A. Egli

(Submitted April 11, 2017; in revised form December 4, 2017; published online January 30, 2018)

In this paper, dendritic growth at the edges of electrogalvanized steel strip has been studied using a specially designed rotating washer electrode which simulates the fluid dynamic conditions and the current density distribution at the steel strip edge found in a production line. The effect of electrolyte pH and current density on dendritic growth in an acidic zinc plating bath ($ZnSO_4$ and H_2SO_4) was addressed. The temperature was kept constant at 60 °C. Solution pH was adjusted to 1, 2 or 3 using different amounts of H_2SO_4. In addition, the influence of temperature on the pH of the solution was determined. The current density was set at 40 or 60 A/dm^2, similar to that used in the industry. Deposits were characterized using SEM and XRD. The results showed that pH strongly affects dendrites shape, length and texture. Furthermore, the morphology of dendrites at the washer edge and of deposits on the flat portion of the washer changed considerably as solution pH was increased from 1 to 3. It was found that the morphology of dendrites at the washer edge stems from the morphology of the deposit on its flat portion, which in turn determines their shape.

Keywords crystal growth, dendrites, electrodeposits, texture, zinc

1. Introduction

Dendritic growth during metal electrodeposition has been studied by many authors since the middle of the twentieth century (Ref 1-7). In general, these studies were focused on theoretical aspects of the phenomenon, which has allowed the development of theories and models that properly fit the experimental evidence.

In spite of the relevance of these results, they have been obtained under static conditions and using very simple geometries while the study of industrial situations, where the formation of dendrites gives rise to quality problems, has not been addressed yet. For example, the occurrence of this type of zinc crystal growth during the continuous electrogalvanizing of steel strip in acid medium usually causes defects that translate into customers' claims or rejections of the product. In these processes, the design of the production lines is performed so that the quality of the material obtained in the flat part of the strip is optimized, while the edges are exposed to high current densities (j) caused by current distribution issues (Ref 8).

Considering this, a cell especially designed to simulate the fluid dynamic conditions and the current distribution at the edge of the steel strip was built. The cell uses a rotating washer electrode (RWE) as cathode. In previous works (Ref 9-11), this system was used to study the influence of j, electrolyte temperature (T), surface finish of the washer edge and its rotation speed (ω) on dendritic growth in an acid zinc plating bath ($ZnSO_4$ and H_2SO_4). The results allowed for the identification of the essential parameters that affect the formation of zinc dendrites and the design of control strategies to diminish or avoid their growth.

It is well known that the pH of the electrolyte can affect the electrogalvanizing process in several ways. For example, for very low pH values corrosion of the line elements increases, which in turn produces a rise in the content of impurities in the bath. Conversely, higher pH values gradually inhibit the chemical dissolution of zinc ingots commonly used to control Zn^{2+} concentration with insoluble anodes technology. Moreover, although acidity of the electrolyte does not modify the average cathodic efficiency of the plating process (Ref 12), the hydrogen evolution reaction (HER) can become important, especially at singularities of the electrode, like the edge of the strip, due to the high current densities found there. With the aim of avoiding pH measuring errors, the functionality of pH with temperature was studied for the $ZnSO_4 + H_2SO_4$ solution employed in this work.

Based on the important and frequent problems generated by dendrite formation in electrogalvanizing industrial lines, it is surprising that the influence of pH in dendritic growth has not been evaluated so far. In the present work, the effect of the electrolyte pH on the generation of dendrites during the electrodeposition of zinc in acidic medium was studied. Morphology and texture changes were also evaluated.

2. Experimental

To conduct the experiments, a RWE especially designed to reproduce the hydrodynamic and current conditions at the steel strip edge was used (Ref 9-11). Figure 1 shows a schematic drawing of the experimental set up. SAE 1010 steel washers were used as substrate (external diameter 40 mm; internal

Leandro N. Bengoa and **Paola Pary**, Centro de Investigación y Desarrollo en Tecnología de Pinturas (CIDEPINT), CICBA-CONICET, Av. 52 e/121 y 122, 1900 La Plata, Argentina and Engineering School, Universidad Nacional de La Plata, Av.1 y 47, 1900 La Plata, Argentina; **Pablo R. Seré** and **Walter A. Egli**, Centro de Investigación y Desarrollo en Tecnología de Pinturas (CIDEPINT), CICBA-CONICET, Av. 52 e/121 y 122, 1900 La Plata, Argentina; and **M. Susana Conconi**, Engineering School, Universidad Nacional de La Plata, Av.1 y 47, 1900 La Plata, Argentina and Centro de Tecnología de Recursos Minerales y Cerámica (CETMIC), CICPBA-CONICET, Cno. Centenario y 506, 1900 La Plata, Argentina. Contact e-mail: l.bengoa@cidepint.gov.ar.

diameter 8 mm). The washers were obtained by laser cutting of steel plates (0.7 mm thickness). They were then mounted on a steel rod isolated with a Teflon cylinder, leaving an exposed area of 0.194 dm^2. A zinc ring with an inner diameter of 70 mm, obtained by casting from an ingot of pure Zn (99.9%), was used as anode (0.660 dm^2).

The solution used in the present study was prepared by dissolving $ZnSO_4 \cdot 7H_2O$ (Biopack, 99.9%) in double-distilled water to reach a concentration of 90 g/l of Zn^{2+}. The electrolyte pH was adjusted at values ranging from 1 to 3 (determined at 60 °C) by addition of H_2SO_4 (Anedra 98%). In previous works in the laboratory, it was found that the electrolyte temperature induces changes in the pH of the electrolyte that are not compensated by the pH meter standard compensation procedure. In this investigation, we measured the pH at different temperatures (20-60 °C) to determine the temperature coefficient of the pH of the electrolyte ($\propto = \frac{\partial pH}{\partial T}$). The pH meter was calibrated before each pH determination at the corresponding temperature.

Zn deposits were obtained galvanostatically controlling the current with a FullEnergy HY3020 DC source. The temperature of the electrolyte was controlled at 60 ± 0.2 °C with a Frigomix 1495 thermostatic bath. The cathodic j was 40 and 60 A/dm^2. Speed rotation was kept constant at 800 rpm in all the experiments. This value was adjusted to obtain a tangential velocity of the fluid at the edge of the RWE equal to the relative speed between the electrolyte and the steel strip in the production line (Ref 9, 10).

It has been previously confirmed that the substrate surface topography plays a major role in the generation of dendrites under conditions of fast moving electrolyte in a similar way as occurs on the static condition (Ref 9, 10). Given that the laser cutting process generates a rough edge that is not representative of those found in the industry, the washers edges were smoothened by a systematic procedure using 80-grit (G80) sandpaper. A medium roughness (Ra) of 0.80 μm (Hommel Tester® T1000 roughness tester) was obtained with this procedure.

Zn deposits were characterized by scanning electron microscopy (SEM), using a Quanta200® FEI (Tungsten filament) equipment. X-ray diffraction (XRD) patterns of zinc dendrites and the deposit on the flat part of the washer were obtained with a goniometer Philips® 3020 PW 3710 using CuKα (λ = 1.54 Å) radiation and a nickel filter. The detector was scanned between 10° and 100° using a 0.04° step and a sampling time of 2 s. The preferential crystallographic orientation was determined through calculation of the texture coefficient for each crystal plane ($TC_{(hk.l)}$) using Eq 1.

$$TC_{(hk.l)} = \frac{I_{(hk.l)}}{I_{0(hk.l)}} \frac{1}{\left[\frac{1}{n}\sum \frac{I_{(hk.l)}}{I_{0(hk.l)}}\right]} \quad \text{(Eq 1)}$$

where $I_{(hk.l)}$ and $I_{0(hk.l)}$ are the intensities corresponding to the planes (hk.l) of sample and standard, respectively (ASTM 4-831 chart for a sample of zinc powder), and n is the number of planes in the diffraction pattern. To evaluate the texture of the dendrites, some of them were detached from the washer, placed on a glass plate and stuck to the plate with double-sided sticking tape. As dendrites are parallel to the surface, their growth direction is parallel to the surface too and their texture will be that of the planes which do not diffract since they are perpendicular to the surface.

Hydrogen formation during electrolysis was measured as a function of pH at j = 40 A/dm^2. A 10-ml burette was turned over the electrolysis cell, and the working electrode was positioned below in order to capture the H_2 generated during the experiment. The burette was filled with the $ZnSO_4$ solution, and the charge spent in H_2 evolution (Q_H) was quantified through the displaced volume of liquid. Cathodic efficiency (CE%) was calculated as the ratio of the net charge of zinc deposition on the total charge during electrolysis (Q_T) (Eq 2).

$$CE(\%) = 1 - Q_H/Q_T \quad \text{(Eq 2)}$$

All experiments were carried out in triplicate in order to verify the reproducibility of the results.

3. Results and Discussion

Figure 2 shows the pH value variation with temperature for three $ZnSO_4$ electrolytes with an initial pH of 1, 2 and 3 (set at

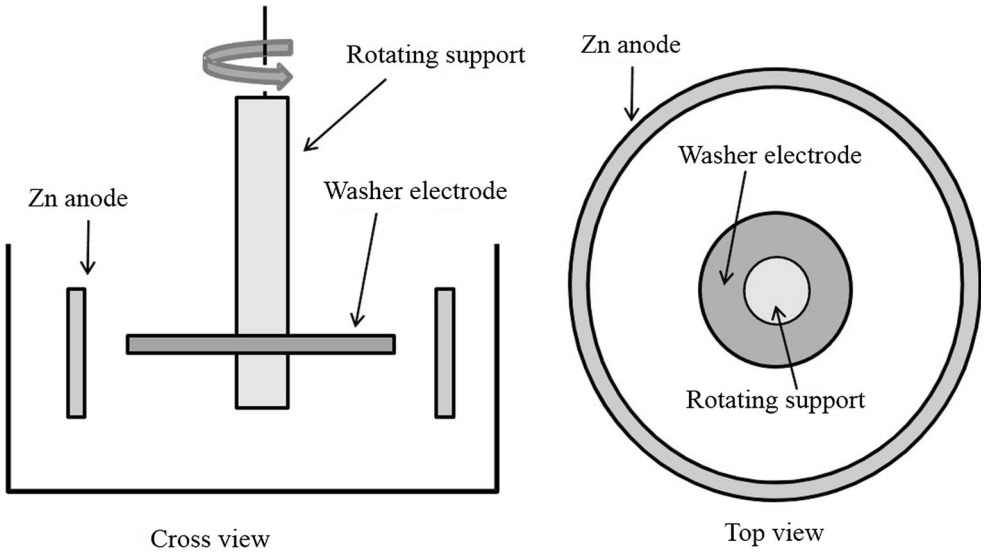

Fig. 1 Schematic drawing of the RWE setup

20 °C). The same linear dependence was found for the three solutions, which can be represented by Eq 3:

$$\mathrm{pH}(T_2) = \mathrm{pH}(T_1) + \alpha(T_2 - T_1) \quad \text{(Eq 3)}$$

where $\alpha = 0.01\ ^{\circ}\mathrm{C}^{-1}$ and T_1 and T_2 are two different temperatures. It is important to recall at this point that this dependence between pH and temperature is not the classic temperature compensation of the glass electrode, but a chemical modification of the equilibrium in solution. Hence, if pH adjustment of the electrolyte is carried out at room temperature (approximately 20 °C) and the zinc electrodeposition is performed at 60 °C, the working pH value will be higher. This experimental fact is very important to adjust the chemical composition of the electrolyte before performing the electrodeposition experiment and has to be considered in automatic process control algorithms.

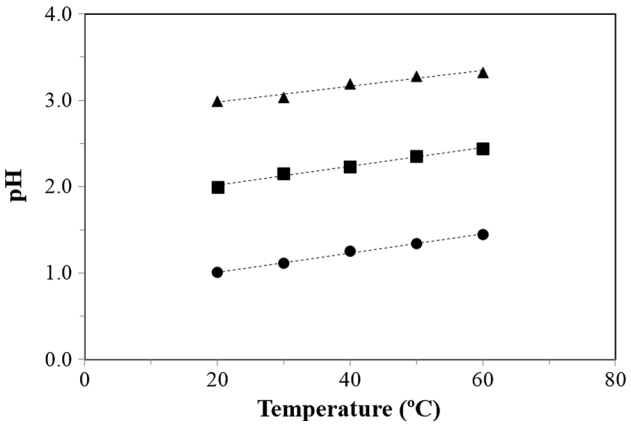

Fig. 2 pH of the electrolyte vs. temperature, black circle represents pH = 1, black square represents pH = 2, and black triangle represents pH = 3

Figure 3 shows the morphology of zinc crystals deposited in the flat part of the electrogalvanized washers at different pH values. It can be observed that at pH = 1 the zinc crystals (named "platelets" due to the fact that their thickness is much lower than their other dimensions) are located with the hexagons parallel to the surface. This morphology stems from a nucleation and growth process which promotes a basal texture, that is, with the planes (00.2) parallel to the surface (Ref 13-16). $TC_{(hk.l)}$ values shown in Table 1 confirm this observation, since a value higher than one of this parameter implies that there is a preferential orientation of that family of planes parallel to the substrate. At pH = 2, the morphology of the crystals did not change substantially. However, as shown in Table 1 a slight increase in the $TC_{(hk.l)}$ of the pyramidal planes is observed and the platelets are slightly tilted. When the pH increases up to 3, the hexagonal crystals are located predominantly inclined with respect to the substrate surface at different angles, presenting a particular morphology where the edges of the platelets are exposed to the surface (Fig. 3). This morphology is known as ridge morphology, and it develops due to the bunching of the microsteps, giving rise to the characteristic macrosteps of this morphology (Ref 15, 17). The latter generates a pyramidal texture (pyramidal planes parallel to the substrate) as a result of the inclination of the Zn platelets

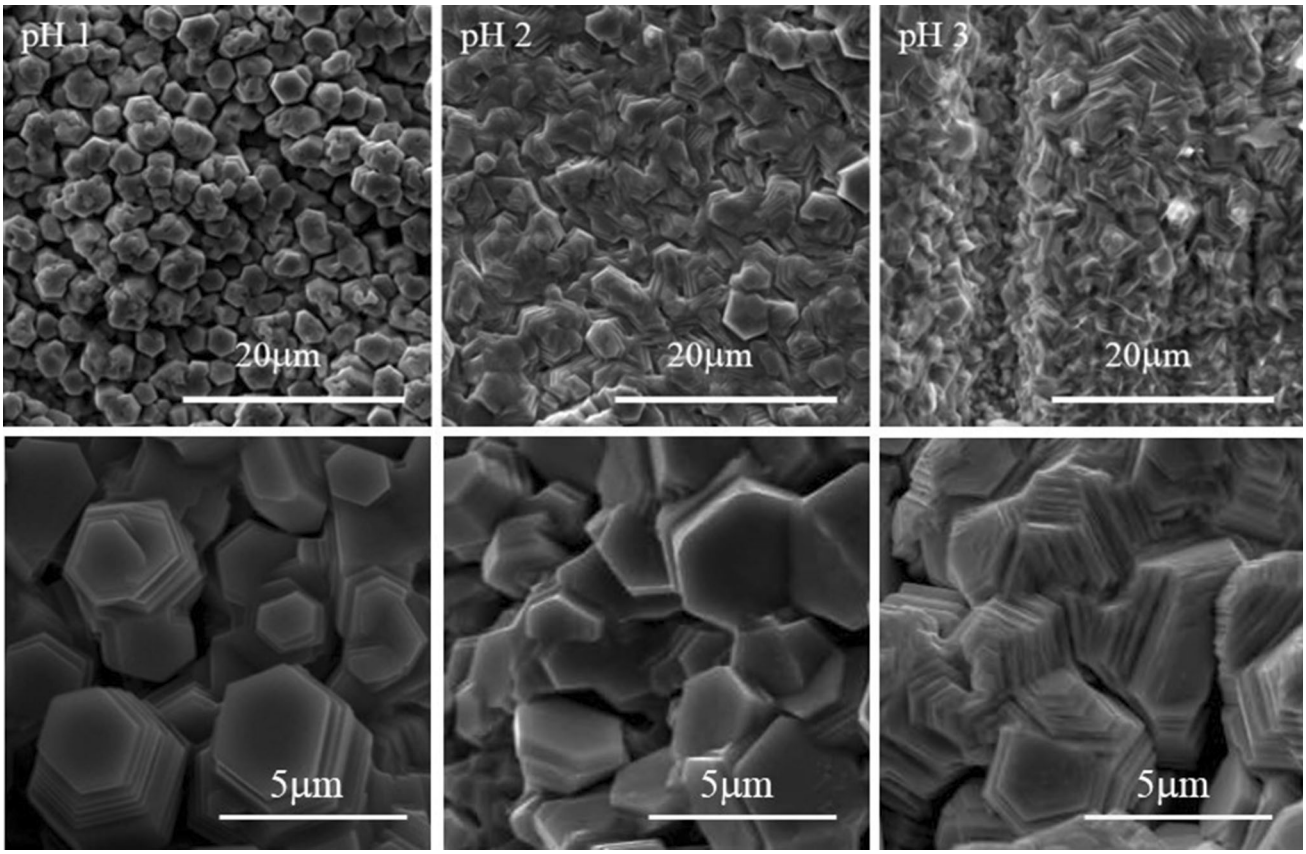

Fig. 3 SEM photographs of the flat part of the disks at different pH values

(Ref 17). For this reason, the sum of the $TC_{(hk.l)}$ values of all pyramidal planes was considered to evaluate the effect of the pH on the texture, that is, (10.1), (10.2), (10.3) and (11.2). The $TC_{(hk.l)}$ of this family of planes increases with increasing pH (Table 1). According to some authors, the transition in the type of nucleation from 3D to 2D that makes the texture and morphology of the zinc coatings change is due to the formation of a zinc hydroxide film on the substrate surface (Ref 13-16). According to these authors, the presence of this compound blocks 3D nucleation sites, promoting the epitaxial growth (2D). However, the authors also highlight that this phenomenon only occurs at low overpotentials, condition under which 3D nucleation is not energetically favorable in systems where the depositing metal exhibits affinity with the substrate (Ref 18-20).

Regarding dendrites, these structures start growing at the edge of the cathode where the current density is higher. These types of deposits grow under activation control at singular points, while the electrode is under mixed or diffusional control. Under these conditions, the reaction rate on the surface of the electrode is limited by the mass transfer rate. In general, this gives rise to coatings that present a globular morphology. However, over certain potential or j values, the presence of small protuberances may promote dendritic growth. These structures are highly regular and crystalline, which is characteristic of an activation-controlled growth.

Table 1 $TC_{(hk.l)}$ of the flat part of the electrogalvanized washers

pH	$TC_{(00.2)}$	$TC_{(sum)} = TC_{(10.1)} + TC_{(10.2)} + TC_{(10.3)} + TC_{(11.2)}$
1	3.59	0.13
2	3.50	1.04
3	2.22	3.88

Dendrites grow maintaining the original morphology of zinc crystals of the flat part of the washer. This implies that at pH = 1, where the hexagons are parallel to the surface, in some singular sites the crystals start to overlap (Fig. 4a) giving rise to a precursor from which the stem of the dendrites will grow. Although dendrites mainly propagate in a direction perpendicular to the basal plane (00.2), secondary branches appear and thrive perpendicular to the main stem (Fig. 4b) forming angles of 60° between each other. This process causes dendrites to acquire a 6-pointed star shape. This morphology is even more discernible when the current density increases (Fig. 5). It is evident that the aspect and growth of this type of deposits is governed by the metal crystalline structure.

When pH is increased to 2, the dendrites start nucleating from crystals that are inclined with respect to the surface (Fig. 4c). As can be seen in Fig. 4(d), dendrites retain the growth inclination and the orientation induced by the morphology of the flat part. At a higher pH, this mechanism becomes more important, the crystals are even more inclined with respect to the surface (Fig. 4e), and as the dendrites grow, they start following random crystallographic orientations, which give dendrites a more globular morphology (Fig. 4f). This fact may be due to the transition of a 2D nucleation mechanism to a 3D mechanism, which is usually observed when coating thickness increases. This behavior has been

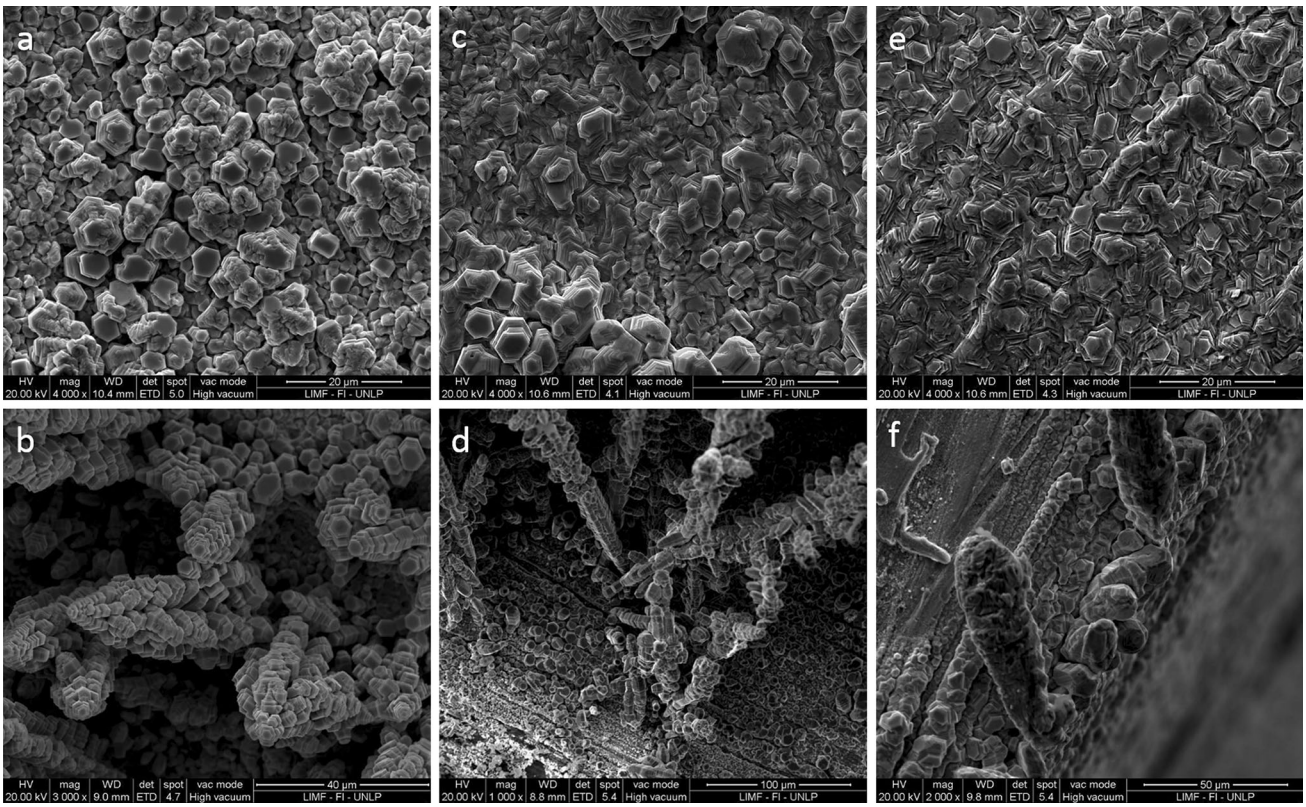

Fig. 4 SEM photograph of zinc-plated washers at 40 A/dm^2: (a) pH 1, flat part; (b) pH 1, edge dendrites; (c) pH 2, flat part; (d) pH 2, edge dendrites; (e) pH 3, flat part; (f) pH 3, edge dendrites

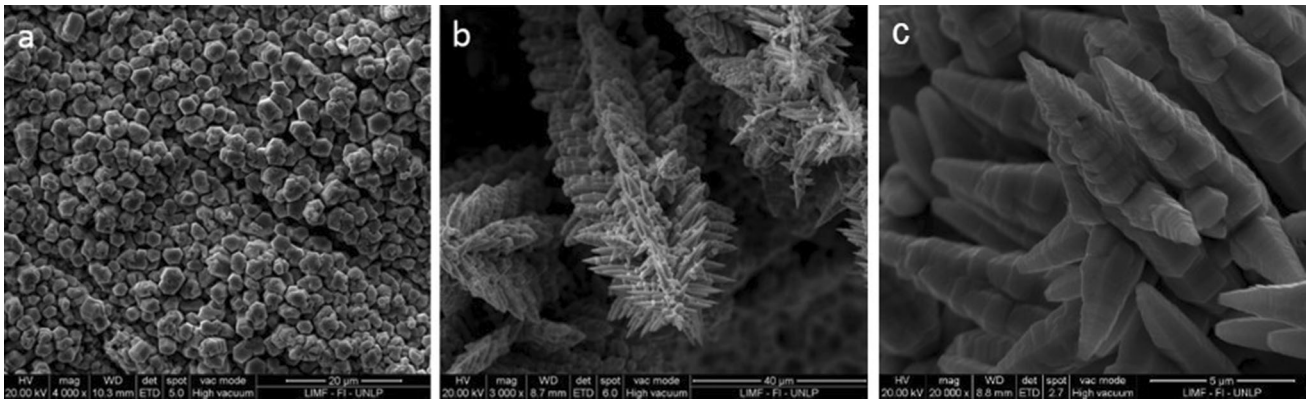

Fig. 5 SEM photograph of zinc-plated washers at 60 A/dm^2: (a) pH 1, flat part; (b) pH 1, edge dendrites; (c) detail of the dendrite (20000X)

Table 2 $TC_{(hk.l)}$ of dendrites

pH	$TC_{(00.2)}$	$TC_{(10.3)}$
1	0.89	2.83
2	1.04	1.78
3	1.37	1.23

observed during the formation of Zn deposits on steel (Ref 17) and corresponds to the Stranski–Krastanov mechanism (Ref 18-20) for systems where the depositing metal exhibits affinity with the substrate, but the misfit between the crystal lattices of both systems is high. This gives rise to strong internal stresses that are alleviated by switching from an epitaxial growth to 3D nucleation.

$TC_{(hk.l)}$ of dendrites obtained at different pH values (Table 2) shows that dendrites have a basal texture for pH = 1, since (00.2) is the plane with the lowest diffraction (low $TC_{(hk.l)}$), in accordance with the morphology of dendrites shown in Fig. 4(b). On the other hand, as pH increases, the dendrites become more pyramidal ($TC_{(10.3)}$ of the parallel oriented dendrites decreases from 2.83 to 1.23). This also agrees with the morphology of the dendrites observed at pH = 3 (Fig. 4f).

William–Hall calculations were done, and a significant dispersion of the data was found. The linear fit of the values was not adequate. According to this, the ordinate would not have a real physical meaning and it would not be correct to calculate the crystal size from those results. It is possible that the deviation from linearity is caused by a marked texture of the samples. Peaks corresponding to plane (002) present a much bigger area than the others. Additionally, the samples present great anisotropy, characteristic of the crystal domains for the dendrites, and the calculation method considers isotropic shapes to obtain a single average diameter in all directions.

Besides, it was observed that the increase in electrolyte pH promotes the formation and growth of longer dendrites (Fig. 6). At pH = 1, only short dendrites can be seen, all of which have a similar size (Fig. 6a). When pH is raised to a value of 2, some dendrites become longer at singular points of the washer edge (Fig. 6b), while at pH = 3 all the perimeter of the washer has long dendrites, giving a haw like aspect to the washer edge (Fig. 6c). This fact is of key importance in the industrial process, since the pH control should be of major concern to avoid the formation of dendrites during the production of electrogalvanized steel strip. One of the reasons that could explain this behavior is the higher hydrogen discharge that is observed at lower pH values as can be seen in Fig. 7. The discharge generates bubbles favoring mass transport toward the electrode by agitation, and hence moving the electrode away from diffusion controlled conditions, necessary for the occurrence of this type of deposits (Ref 4). Due to the higher contribution of hydrogen evolution reaction to the total current, at the higher current densities found on the strip edge, the current of Zn deposition will be lower, reducing the possibility of dendrite formation.

4. Conclusions

A linear relationship between the pH of the electrolyte and the temperature was found. This allows the calculation of the pH of $ZnSO_4$ solutions for different process temperatures. Due to this behavior, it becomes necessary to take in consideration the temperature of the solution when measuring its pH value. This is important when automatic process control is considered. From the results obtained in the present work, we can infer that if the electrogalvanizing process is carried out at low pH, the nucleation of hexagonal crystals of Zn is of 3D type, which generates a morphology with the basal planes parallel to the surface. At higher pH values, the nucleation mechanism varies, changing to 2D, which promotes the epitaxial growth and generates a laminar morphology called ridge, with zinc crystals inclined with respect to the substrate. As a result, the texture of the deposit is pyramidal. The type of nucleation and growth of the crystals are essential in the determination of the morphology that the dendrites formed at the disks edges will have: At low pH, the growth is more homogeneous with a morphology that reflects the hexagonal structure of the Zn. Conversely, dendrites that are formed from the inclined crystals (pyramidal) at higher pH grow by overlapping of crystals randomly orientated as a result of a transition in the nucleation mechanism. This generates less directional dendrites with globular shapes. On the other hand, the pH has a marked influence on the amount and length of dendrites formed.

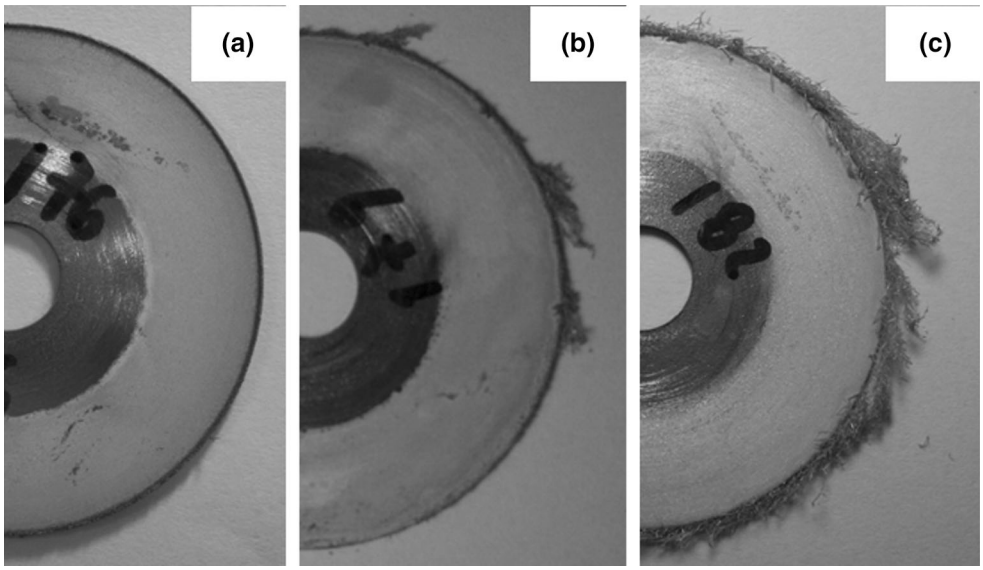

Fig. 6 Photographs of electrogalvanized samples (a) pH = 1, (b) pH = 2 and (c) pH = 3

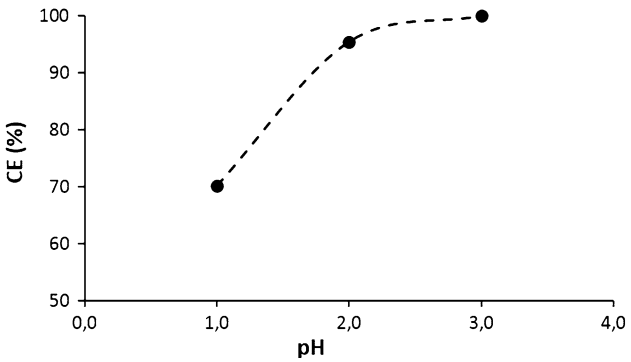

Fig. 7 Cathodic efficiency as a function of pH (j = 40 A/dm^2)

Acknowledgments

The authors would like to acknowledge the Comisión de Investigaciones Científicas de la Provincia de Buenos Aires (CICPBA), Consejo Nacional de Investigaciones Científicas y Técnicas (CONICET) and Universidad Nacional de La Plata (UNLP) for their financial support to this work.

References

1. G. Wranglén, Dendrites and Growth Layers in the Electrocrystallization of Metals, *Electrochim. Acta*, 1960, **2**(1-3), p 130–143
2. J.L. Barton and J.O.M. Bockris, The Electrolytic Growth of Dendrites from Ionic Solutions, *Proc. R. Soc. Lond. A*, 1962, **268**(1335), p 485
3. S.W. Watson and R.P. Walters, The Effect of Chromium Particles on Nickel Electrodeposition, *J. Electrochem. Soc.*, 1991, **138**(12), p 3633–3637
4. N.D. Nikolić and K.I. Popov, A New Approach to the Understanding of the Mechanism of Lead Electrodeposition, *Electrodeposition and Surface Finishing: Fundamentals and Applicationsed*, S.S. Djokić, Ed., Springer, New York, 2014, p 85–132
5. N.D. Nikolic and K.I. Popov, *A New Approach to the Understanding of the Mechanism of Lead Electrodeposition*, Electrochemical Production of Metal Powdersed Springer, New York, 2012, p 1–62
6. L. Avramović, M.M. Pavlović, V.M. Maksimović, M. Vuković, J.S. Stevanović, M. Bugarin, and N.D. Nikolić, Comparative Morphological and Crystallographic Analysis of Electrochemically- and Chemically-Produced Silver Powder Particles, *Metals*, 2017, **7**(5), p 160
7. T.N. Ostanina, V.M. Rudoi, A.V. Patrushev, A.B. Darintseva, and A.S. Farlenkov, Modelling the Dynamic Growth of Copper and Zinc Dendritic Deposits Under the Galvanostatic Electrolysis Conditions, *J. Electroanal. Chem.*, 2015, **750**, p 9–18
8. N. Ibl, Current Distribution, Comprehensive Treatise of Electrochemistry, *Electrodics: Transported*, E. Yeager, J.O.M. Bockris, B.E. Conway, and S. Sarangapani, Ed., Springer, New York, 1983, p 239–315
9. L.N. Bengoa, S. Bruno, H.A. Lazzarino, P.R. Seré, and W.A. Egli, Study of Dendritic Growth of Zinc Crystals on the Edges of Steel Sheet, *J. Appl. Electrochem.*, 2014, **44**(12), p 1261–1269
10. L.N. Bengoa, S. Bruno, H.A. Lazzarino, P.R. Seré, and W.A. Egli, Dendritic Zinc Growth on the Edges of Flat Steel Strip During Electro Galvanizing, *Procedia Mater. Sci.*, 2015, **8**, p 1174–1183
11. L.N. Bengoa, P.R. Seré, M.S. Conconi, and W.A. Egli, Morphology and Texture of Zinc Deposits Formed at the Edge of a Rotating Washer Electrode, *J. Mater. Eng. Perform.*, 2016, **25**(7), p 2936–2942
12. D.R. Gabe, The Role of Hydrogen in Metal Electrodeposition Processes, *J. Appl. Electrochem.*, 1997, **27**(8), p 908–915 (in English)
13. K.R. Baldwin, C.J.E. Smith, and M.J. Robinson, Study into the Electrodeposition Mechanisms of Zinc-Nickel Alloys from an Acid-Sulphate Bath, *Trans. Inst. Met. Finish.*, 1994, **72**(2), p 79–88
14. T. Tsuru, S. Kobayashi, T. Akiyama, H. Fukushima, S.K. Gogia, and R. Kammel, Electrodeposition Behaviour of Zinc-Iron Group Metal Alloys from a Methanol Bath, *J. Appl. Electrochem.*, 1997, **27**(2), p 209–214
15. X.-L. Gu, Y.-Q. Shan, J. Liang, and C.-S. Liu, Morphology and Texture of High Speed Galvanized Coatings on Interstitial Free Steel Sheet, *Trans. Nonferr. Metal Soc. China*, 2011, **21**(3), p 488–492
16. A.R. Despić and K.I. Popov, *Modern Aspects of Electrochemistryed*, ed by B.E.C.a.J.O.M.B Editors (1972), pp. 304–310
17. K. Raeissi, A. Saatchi, M.A. Golozar, and J.A. Szpunar, Texture and Surface Morphology in Zinc Electrodeposits, *J. Appl. Electrochem.*, 2004, **34**(12), p 1249–1258
18. N. Kanani, *Electroplatinged*, ed. by N.K. Editor. (Elsevier, New York, 2004), pp. 141–177
19. Y. Gamburg and G. Zangari, *Theory and Practice of Metal Electrodepositioned*, Springer, New York, 2011, p 97–122
20. R. Liu, A.A. Vertegel, E.W. Bohannan, T.A. Sorenson, and J.A. Switzer, Epitaxial Electrodeposition of Zinc Oxide Nanopillars on Single-Crystal Gold, *Chem. Mater.*, 2001, **13**(2), p 508–512